Synthesis and Physical Property Exploration of $LaNiGa_2$

Henry Bowman

UC Davis Physics REU Summer 2022, Professor Valentin Taufour

Abstract

$LaNiGa_2$ is an unconventional superconductor that breaks time-reversal symmetry (TRS). As a material that could host quasiparticle Majorana fermions (particles that are their own antiparticles), there is significant potential for $LaNiGa_2$ in quantum computing. Until recently, studies of $LaNiGa_2$ have been limited to polycrystalline samples. This is no longer true: using a flux growth technique, single-crystal $LaNiGa_2$ has been produced. This advancement has already resulted in an improved understanding of the $LaNiGa_2$ unit cell and is expected to enable further research about this material and its properties. This paper describes two attempts to learn more about the behavior and properties of $LaNiGa_2$. First, this paper details the preparation of a $LaNiGa_2$ mosaic for an experiment using muon spin resonance (μSR). The goal of this experiment is to identify TRS breaking in $LaNiGa_2$ in the form of an internal magnetic field that appears at the onset of superconductivity. Second, measurements of the resistivity of $LaNiGa_2$ across temperatures are reported. These measurements indicate that resistivity, and possibly $LaNiGa_2$ impurities, could vary based on crystallographic axis. This paper also includes a brief overview of $LaNiGa_2$ synthesis and its challenges, as well as areas for future study with this material.

1 Background and Motivation

1.1 Significance of $LaNiGa_2$

$LaNiGa_2$ is an intermetallic compound. A recent paper from Badger et al. (2022) identified the space group of $LaNiGa_2$ as *Cmcm*, a designation describing the symmetries present in the $LaNiGa_2$ unit cell [1]. Two features of the *Cmcm* space group that are significant for $LaNiGa_2$ are the glide plane (simultaneous reflection and translation) and screw-axis (simultaneous rotation and translation) symmetries. Applying these symmetry operations leaves no fixed points in the $LaNiGa_2$ unit cell. As a result, these symmetries of the unit cell cause significant electron degeneracy in $LaNiGa_2$—if an electron is subject to a given potential at one location in the unit cell, it will be subject to the same potential at other locations as determined by

the glide plane and screw axis. Specifically, there exist points of overlap between different Fermi surfaces (the surfaces in energy space resulting from bands that include the Fermi energy) in $LaNiGa_2$. In effect, this means that the highest-energy electrons in $LaNiGa_2$ from different bands are degenerate [1].

This electron degeneracy in $LaNiGa_2$ makes it a "topological material"—since the degeneracy results from symmetries in the unit cell, the building block of $LaNiGa_2$ crystals, it isn't dependent on the size or shape of the sample in question. The so-called "topological features" of $LaNiGa_2$, the points of degeneracy between different Fermi surfaces, significantly impact the superconductivity of $LaNiGa_2$. In "conventional" superconductors, two electrons from the same energy band with opposite spin become coupled through lattice vibrations. The new composite quasiparticle (called a "Cooper pair" after theorist Leon Cooper) condenses to a lower-energy state where it traverses the material with no resistance [2]. In $LaNiGa_2$, typical Cooper pairs do not form; instead, electrons from different intersecting Fermi surfaces become coupled. Since the electrons come from different bands (in effect), there is no restriction that they must have opposite spin (as is the case with Cooper pairs), and pairs form between electrons with the same spin. Thus, the superconducting pairing state is a "spin-triplet," given the three possibilities for electrons with the same spin (both spin up, both spin down, and $1/\sqrt{2}$ of each). This spin-triplet pairing state is what classifies $LaNiGa_2$ as an unconventional superconductor, and directly results from the normal-state (i.e., above T_c) topological features and symmetries of the unit cell. $LaNiGa_2$ (and other superconductors with normal-state topological features) are of significant interest because they could host Majorana fermions as quasiparticles. Majorana fermions (which are their own antiparticles) have proven elusive as of yet, but if discovered, they could make stable qubits [3]. The prospect of improved quantum computing incentivizes research on topological superconductors, such as $LaNiGa_2$.

1.2 Magnetic Properties of Conventional and Unconventional Superconductors

The phenomenon of superconductivity is closely tied to magnetism. All known superconductors display the Meissner Effect, in which a superconductor expels any external magnetic field from its bulk. Therefore, a superconductor is a perfect diamagnet. This result is easily observable in a setup with a superconductor and a small permanent magnet, where the permanent magnet is placed on top of the superconductor. When the superconductor is in its normal state, the permanent magnet rests on top of it. As the superconductor is cooled below T_c, it expels all the magnetic flux from its bulk, counteracting the field from the permanent magnet. Since the superconductor's internal magnetic field opposes that of the permanent magnet, the two repel and the permanent magnet floats above the superconductor, defying gravity. In effect, this means that the superconductor acquires a magnetization such that the total magnetic field inside of it is 0: $B = \mu_0(H +$

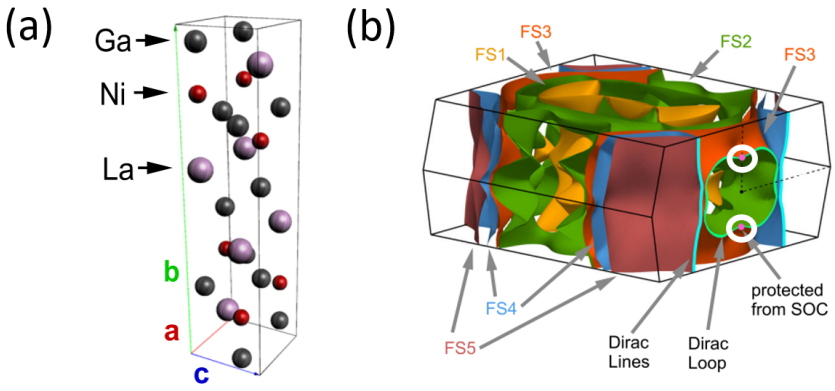

Figure 1: Panel (a) shows the unit cell of $LaNiGa_2$. This is the building block of the macroscopic crystal; all unit cells are aligned in a single crystal sample. Panel (b) shows the Fermi surfaces of $LaNiGa_2$, which result from electron bands in which the Fermi Energy is contained. Of note are the points of degeneracy between Fermi surfaces (shown in pink and circled in white) that allow the unconventional superconducting state to form. Both panels taken from source [1].

M) = 0, where H is the applied magnetic field. (A related quantity, χ, is defined as M/H and is a measure of sample quality: a perfect superconductor exactly cancels out the external field, so χ = -1.)

Although the mechanism is different, the result of the Meissner Effect is similar to that of an electric conductor in an external electric field, in which the free charges in the conductor migrate to completely cancel out the external field. The Meissner Effect, and the superconducting state in general, is dependent on temperature: above the transition temperature, the superconductor is in its normal state and does not expel any magnetic flux. In general, superconductivity is temperature-dependent because it involves interactions between electrons mediated by lattice vibrations (phonons) in a material. Higher temperatures correspond to random lattice vibrations that interfere with favorable electron-electron interactions, making superconductivity impossible.

The strength of the external magnetic field plays a role as well: a given material can only counteract an external magnetic field of a given strength before the superconducting state is broken. An explanation for this phenomenon goes as follows: only a small fraction of the electrons in a material participate in superconductivity [2]. Therefore, only a limited current strength can be achieved to counteract an external magnetic field before the external field predominates and determines the behavior of electrons in the material. In some superconductors (called type I), this effect happens immediately—once the critical field strength is reached, all magnetization disappears. In others, like $LaNiGa_2$ (called type II), the destruction of the superconducting state is gradual: at the first critical field, the strength of the magnetization $|M|$ exponentially decreases, only

reaching 0 by the second critical field. The critical field (or fields, on a type II superconductor) are intrinsic to the material. Figure 2 shows a plot of $|M|$ for both types of superconductors. The magnetization and internal magnetic field in a superconductor are determined by the strength of the external field, up until the critical field is reached. At higher fields, the superconducting state disappears or decays, and magnetization eventually drops to 0. The Meissner Effect is a hallmark of superconductivity—the magnetic susceptibility χ indicates the completeness of the superconducting transition—and thus it is used to examine sample quality, as described in Section 3.1.

While in the superconducting state, most superconductors do not display magnetization beyond that which occurs due to the Meissner Effect, however. (Other types of magnetization unrelated to superconductivity, like that due to orbital angular momentum, may be present.) $LaNiGa_2$ may be different from other superconductors in this way: Hillier et al. (2012) reported a magnetic anomaly in $LaNiGa_2$ upon the superconducting transition—see Figure 2. One possibility is that $LaNiGa_2$ produces an extra internal magnetic field, perhaps due to spin magnetization, at the onset of superconductivity [4]. This result provided preliminary experimental justification for the TRS-breaking nature of $LaNiGa_2$. However, since Hillier et al. used polycrystalline $LaNiGa_2$ (in which unit cells are not aligned on a macroscopic scale), the exact nature of the TRS breaking is not fully understood. Given that single-crystal $LaNiGa_2$ can now be grown, an obvious next step in researching $LaNiGa_2$ is to try to better understand this magnetic response, which is assumed to be responsible for $LaNiGa_2$'s TRS breaking. By using single-crystal $LaNiGa_2$, it may be possible to determine the strength and orientation of this TRS-breaking field, for example.

1.3 Relevance of Resistivity Measurements

Measuring the resistivity of a superconductor is a clear way to observe the superconducting transition: Below T_c, resistivity will drop to 0. Observing superconductivity through resistivity can augment magnetic susceptibility measurements. Although $LaNiGa_2$ is important primarily because of its superconductivity (when resistivity is 0), studying the nonzero resistivity of $LaNiGa_2$ in its normal state is telling as well. There are several sources of resistivity in $LaNiGa_2$, some of which persist at low temperatures and thus influence superconductivity. Since $LaNiGa_2$ is an intermetallic compound, the Fermi energy falls in the middle of multiple electron bands (evidenced by the existence of Fermi surfaces in $LaNiGa_2$). As a consequence, resistivity drops with temperature, because at lower temperatures phonons are suppressed and electrons scatter less. According to the Block-Gruniesen model, electron-phonon scattering is proportional to T^5, and is the dominant mechanism for resistivity in $LaNiGa_2$ at temperatures above 10 K [3]. At low temperatures, resistivity occurs due to electron-electron scattering and defect scattering. Electron-electron scattering has a

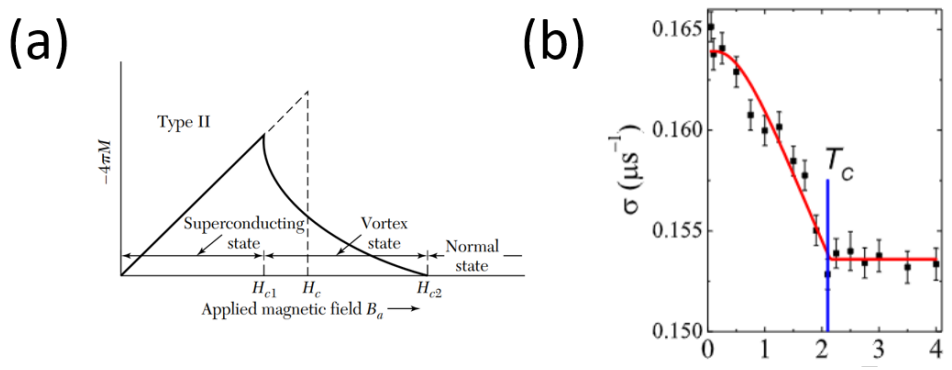

Figure 2: Panel (a) shows the magnetization, M, of a type II superconductor like $LaNiGa_2$ as a function of applied magnetic field H, taken from source [2]. Below the first upper critical field H_{c1} (at which vortices begin to form), the magnetization increases linearly with field strength—measuring the magnetic susceptibility of $LaNiGa_2$ utilizes this property. Panel (b) shows a key result of Hillier et al. 2012 depicting the unconventional magnetic response of $LaNiGa_2$ [4]. σ, the Pauli matrix vector that represents the interaction between spin and an external electromagnetic field, clearly changes at T_c, evidence of the TRS-breaking internal magnetic field.

T^2 dependence, while defect scattering is independent of temperature. Near the superconducting transition at about 2 K, electron-phonon and electron-electron scattering are negligible, only defect scattering remains. Taking measurements of resistivity as a function of temperature can reveal information about sample quality. Specifically, the residual resistivity ratio (RRR) compares resistivity at room temperature (where electron-phonon scattering dominates) to resistivity at just above T_c (ρ_0, where only defect scattering remains), RRR = ρ(300 K) / ρ_0. High RRR values correspond to fewer defects and are generally accepted as an indication of high-quality samples.

Previous unpublished work with single-crystal $LaNiGa_2$ prompted some confusion: different samples displayed different values of RRR and ρ_0 (resistivity just above T_c) by up to a factor of 2. Given the uniformity of samples obtained via flux growth, this result defies expectations. Resistivity should be a property intrinsic to the material, not sample-dependent. The initial motivation behind measuring $LaNiGa_2$ resistivity was to prepare for an electron irradiation experiment. In this technique, a sample is bombarded with high-energy electrons to create vacancies in the lattice. The effect of these vacancies on resistivity can then be determined by comparing resistivity before and after irradiation. This can give a general sense of how resilient a material is to radiation. In order to effectively compare the effects of electron irradiation, it is necessary to obtain a collection of samples with uniform resistivity—a collection unlike the samples previously tested. Therefore, a major goal in taking $LaNiGa_2$ resistivity measurements was to

produce a collection of samples with uniform resistivity, and to determine whether the previous discrepancy in resistivity was anomalous or if it could be observed again. Since resistivity measurements also provide evidence of superconductivity and inform sample quality, as described above, studying resistivity is a useful endeavor.

2 Synthesis of $LaNiGa_2$ and Associated Challenges

Single-crystal $LaNiGa_2$ samples studied in this paper were prepared using a Gallium-deficient self-flux technique. To begin, precursors were weighed out according to the stoichiometric ratio $La_{33}Ni_{33}Ga_{34}$. The precursors were then arc-melted into a homogeneous, eutectic mixture in an oxygen-free environment, and the mixture was crushed into small pieces and loaded into an alumina (AlO_3) Canfield crucible. Next, the crucible was placed in a quartz ampoule, which was partially backfilled with Argon (to a pressure of 170 mTorr) and sealed. Evacuating the ampoule in this step and arc-melting the precursors in an oxygen-free environment were crucial steps for ensuring that crystal growth occurred in the absence of oxygen. Oxygen readily reacts with Lanthanum and can act as a nucleation site for crystals, resulting in incorrect stoichiometric ratios and numerous small crystals, respectively. After sealing, the ampoule was placed in a furnace. The furnace heated to a temperature of 1150 C and remained there for eight hours, and then slowly cooled to 800 C over a period of 100 hours. At 1150 C, the homogenous precursor mixture melts. As it cools, the mixture becomes supersaturated and $LaNiGa_2$ crystals begin to form, with excess Lanthanum and Nickel acting as a flux. At 800 C, the ampoule is removed from the furnace, rapidly inverted, and centrifuged to separate the crystals from the flux before it solidifies. More details about the flux-growth technique for $LaNiGa_2$, including a discussion of flux choice, and effects of precursor stoichiometry and heating profiles on crystal growth can be found in [3]. After the growth is complete, crystals can be characterized via Powder X-Ray Diffraction, a technique that uses Bragg's Law of Diffraction to produce a unique spectrum (of intensity as a function of incident x-ray angle) for each crystal structure.

When $LaNiGa_2$ growth is successful, single-crystal samples with surface area between 1 and 25 mm^2 can be obtained. These samples are high-quality, with RRR values of about 10, and produce orderly Laue diffraction patterns, evidence of neatly aligned unit cells throughout the entire macroscopic crystal (the Laue diffraction method will be described more in Section 3.1). These samples are platelike in appearance with the crystallographic b-axis perpendicular to crystal face [1]. However, producing these platelike, high-quality crystals proves difficult. Temperature gradients within an individual furnace can significantly influence crystal growth: two samples prepared identically but situated at different points in the furnace produce crystals with markedly different morphology and qualities. For example, an ampoule in the middle of one

specific furnace yielded platelike crystals with higher RRR and T_c values, while an ampoule in the front of the same furnace produced stacked, terraced crystals with lower values of RRR and T_c [3]. Differences between furnaces also play a complicating role. Most successful $LaNiGa_2$ growths came from the furnace "Haddock," but since the Taufour lab group moved to a new space in 2022, that furnace has been decommissioned and replaced by a newer furnace, "Kuttus." Regardless of placement within "Kuttus," most batches produce terraced crystals. As mentioned by Badger (2021), "the temperature gradient within the furnace itself can have a dramatic impact on the growth of the crystals. Although the temperature control system may state that entire volume of a furnace is at a uniform temperature, convection currents and temperature gradients will always occur and vary between furnaces," [3]. The mechanism by which temperature gradients and differences between furnaces affect crystal growth is relatively unknown; the large number of uncontrollable factors makes understanding the issue a daunting task. Laue diffraction reveals that terraced crystals have a different macroscopic arrangement of unit cells than platelike crystals—the general idea is that in platelike $LaNiGa_2$, the b-axis grows perpendicular to the largest surface area of the crystal. In terraced $LaNiGa_2$ however, the b-axis is oriented along the length of the crystal instead of normal to the largest exposed crystal face. More details are given in Section 3.1. Furnace specifics are not only poorly understood, but also very important to the crystal growth process.

I attempted three growths of $LaNiGa_2$ during my time at UC Davis following the steps given in this section; ultimately, all three were unsuccessful. The first and third attempts produced heavily terraced crystals with poor magnetic susceptibility values. The second attempt produced a different compound entirely, $LaGa_2$. This attempt was different from the other two because the growth took place in a crucible made of Tantalum, a metal with a very high melting point that is entirely inert during crystal growth. By contrast, a small portion of the oxygen in the alumina crucible used for the first and third synthesis is not inert, and reacts with some of the Lanthanum in the molten mixture. This produces a small but non-negligible "shell" of Lanthanum Oxide (La_2O_3) along with $LaNiGa_2$. Since some of the Lanthanum forms the shell, the exact stoichiometry of the mixture is not $La_{33}Ni_{33}Ga_{34}$—the proportion of Lanthanum is smaller and the proportions of Nickel and Gallium are larger. The modified stoichiometry as a result of La_2O_3 shell formation is favorable for $LaNiGa_2$ growth: when the shell forms, so does $LaNiGa_2$. However, in the Tantalum crucible, none of the Lanthanum oxidized, and thus the stoichiometry of the mixture was not favorable for $LaNiGa_2$. If growths are to be attempted in a Tantalum crucible again, slightly less Lanthanum should be used to simulate the amount that is lost to oxidation in an alumina crucible. Successful $LaNiGa_2$ growth is very sensitive to exact precursor stoichiometry as well as furnace characteristics. As a result of my unsuccessful synthesis attempts, I used samples created by a graduate student in the lab group, Davis Zackaria, for the measurements described in the following section.

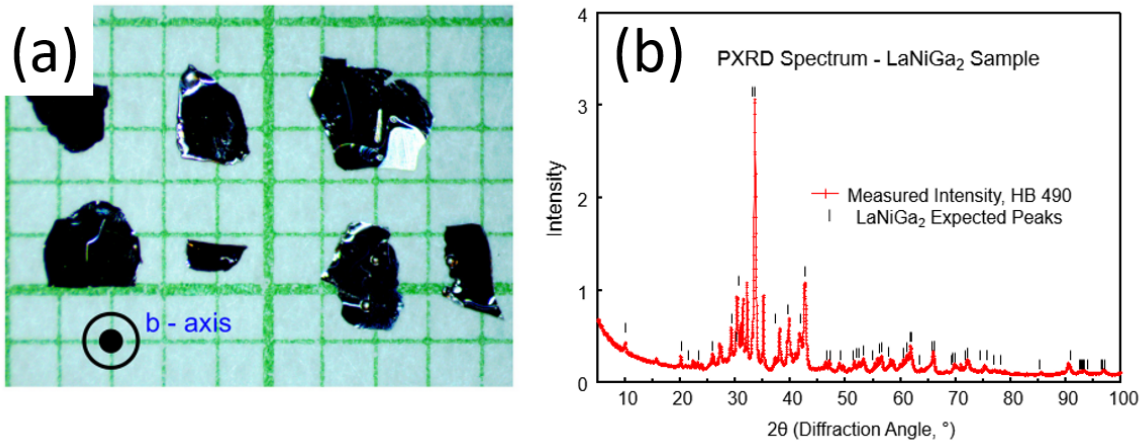

Figure 3: Panel (a) shows high-quality single-crystal $LaNiGa_2$, taken from source [1]. Of note, the b-axis grows perpendicular to the crystal face in this platelike morphology (compare with terraced crystals shown in Figure 4). Panel (b) shows an example PXRD plot with measured intensity peaks alongside calculated peaks based on $LaNiGa_2$ structure.

3 Physical Measurements: Techniques, Results, and Discussion

As collective understanding of materials improves and experiments grow ever more sophisticated, individual labs take on increasingly limited roles in the research process. Successful experimentation often requires cooperation between several lab groups, each of which carries out a specific subset of tasks. The Taufour lab group specializes in material synthesis, characterization, and preliminary measurements. This work is often done in preparation for more complicated experiments completed by collaborators. This section describes work done in preparation for two further experiments with $LaNiGa_2$: first, a search for the TRS-breaking internal magnetic field using μSR, and second, an investigation into the effects of electron irradiation and lattice vacancies on resistivity. Although both of these secondary experiments are beyond the scope of the Taufour lab, significant work goes into preparing for these experiments. The lead-up to the μSR experiment is described first with details about resistivity measurements given second.

3.1 $LaNiGa_2$ Mosaic Production

$LaNiGa_2$ is a TRS-breaking superconductor based on the symmetry operations present in its unit cell alone, but experimental evidence of this quality can come from successfully detecting an internal magnetic field with μSR. A general description of the μSR experiment goes as follows: a sample of the material being studied is placed in the path of a spin-polarized positive muon beamline. Positive muons are unstable; they

decay into a positron and various neutrinos with a mean lifetime of about 2 microseconds after production. The spin-polarized positive muons precess with a frequency ω, but if they interact with a magnetic field, this precession frequency changes. As a result, positrons are emitted preferentially in one direction more than another. Positron detectors are positioned in front of and behind the sample, and their count rates can reveal the presence of even minuscule magnetic fields.

For a μSR experiment to be successful, the sample must be sufficiently thick for positrons to become implanted and interact with an internal magnetic field, if present. The sample also should be as large in area as the beam so that as many muons from the beam as possible interact with the material. This guarantees robust data. The μSR beamline used to examine $LaNiGa_2$ is about 14 mm in diameter, yet even the largest individual $LaNiGa_2$ crystals are only a few millimeters in length. Thus, preparing an effective sample for the beamline involved assembling a mosaic of about two dozen $LaNiGa_2$ crystals, all of requisite thickness and aligned with each other. Assembled properly, the mosaic simulates a single $LaNiGa_2$ crystal that is much larger than what can be grown in the Taufour Lab. The first step in creating the $LaNiGa_2$ mosaic was to identify samples that were large in surface area and thick, this was done by visual inspection. Given their greater uniformity and better quality than terraced crystals, only platelike $LaNiGa_2$ was used in the mosaic—more details on this decision will be given shortly. After preliminary samples were identified visually, their surface mass density was measured. This entailed measuring the surface area of the platelike crystal face using computer software and taking the mass of the crystal, acceptable crystals were ones with > 140 mg of mass for each cm^2 of surface area. Given the density of $LaNiGa_2$, this corresponds to crystals at least 0.2 mm thick (0.2 mm is the maximum penetration depth of the muon beamline).

Once the thickness of crystals was verified, the magnetic susceptibility and T_c were measured using the Magnetic Property Measurement System (MPMS). Taking this measurement involved affixing the sample to a mylar strip and placing the strip inside a standard plastic drinking straw. The sheet/straw apparatus was then loaded into the chamber of the MPMS, which was evacuated and brought down to a temperature around 10 K (above T_c for $LaNiGa_2$). Then a small magnetic field (normally 10 Oe) was applied, and the sample was moved vertically through the sample space, which contained several magnetic sensors. Given the applied external field, the sample (if superconducting) would acquire a magnetization opposing the external field, per the Meissner Effect. As the sample moved relative to the sensors, the net magnetic field received would change, allowing the magnetic response of the sample to be quantified. Above T_c, $LaNiGa_2$ has little magnetic activity, and hence magnetic susceptibility is very close to 0. Below T_c however, a high-quality sample would be expected to acquire a magnetic susceptibility value close to or at -1. The susceptibility value served as an indicator of the proportion of the sample that was superconducting: for example, a susceptibility of -0.5 below T_c signifies that half of the sample obeys the Meissner Effect, while the other half is still in its

normal state. For the μSR experiment, samples had to have a susceptibility value less than -0.8, that is, at least 80% of the bulk had to be superconducting. Again, this requirement was imposed so that there was the greatest possible chance of interaction between decaying muons and superconducting $LaNiGa_2$.

The next steps in preparing the $LaNiGa_2$ mosaic were polishing and cutting. The goal of polishing crystals was to establish a flat face to fasten to the backing plate for the mosaic. Cooling of the sample happened via contact with the backing plate, so establishing a flat face with large surface area was crucial to ensuring that the entire sample be cooled, and thus enter the superconducting state. Although polishing proved to be a delicate task in practice, it was fairly simple in theory: crystals were affixed to a small piece of metal (using Crystalbond adhesive) and then the exposed face was sanded using very fine sandpaper. Once a flat face was established, the crystal was washed in acetone to remove traces of the adhesive. Following the polishing step, some crystals were cut using a simple box cutter blade to remove thin portions or to create a more uniform crystal shape. The final step before mosaic assembly was alignment using a Laue diffractometer. The goal of this step was to align the crystallographic axes in all the samples to effectively simulate one much larger crystal. This step relies on the advantage posed by growing single crystals: with a polycrystalline sample, aligning all the unit cells at a macroscopic scale is impossible. Laue diffraction uses an x-ray beam to produce a characteristic back-scatter pattern depending on crystallographic orientation. Since the platelike crystals grow with the b-axis perpendicular to the face, only the a- and c-axes needed aligning. Determining the pattern corresponding to each orientation involved modeling using computer software. Once a diffraction pattern was obtained for each possible orientation, crystals were aligned and fastened to a silver backing plate. The completed mosaic was then sent to collaborators in Canada with access to a muon beamline at TRIUMF.

During the Laue diffraction process, an important difference between platelike and terraced samples became evident: the crystallographic orientation differs between these two types of crystals. In platelike samples, the b-axis is perpendicular to crystal face, and crystals tend to grow with the plates as their largest surface area. Therefore, with platelike crystals laying flat in a natural position, the b-axis points vertically up and down. However, in terraced samples, the b-axis is horizontal to the largest surface area on the crystal (likely due to furnace characteristics, as mentioned in Section 2). This was discovered when terraced crystals were cleaved along the individual steps and then aligned using the Laue diffractometer. The individual steps that compose the terraced crystal produced Laue diffraction patterns like the platelike crystals, indicating that each step constitutes a small plate (like the plates in the first type of crystal). However, the plates are stacked horizontally, almost like slices in a loaf of bread. Not only are the platelike crystals different from terraced crystals in visual appearance, their macroscopic crystallographic orientation is also different. To visualize this difference, compare the crystals in Figure 3, Panel (a) and Figure 4, Panel (d). It remains

unclear how furnace differences and temperature gradients are responsible for altering the crystallographic orientation of crystals during nucleation.

All told, 24 $LaNiGa_2$ crystals went into the completed mosaic, I worked on about half. This process involved taking over 130 measurements of surface mass density and about 20 measurements of magnetic susceptibility.

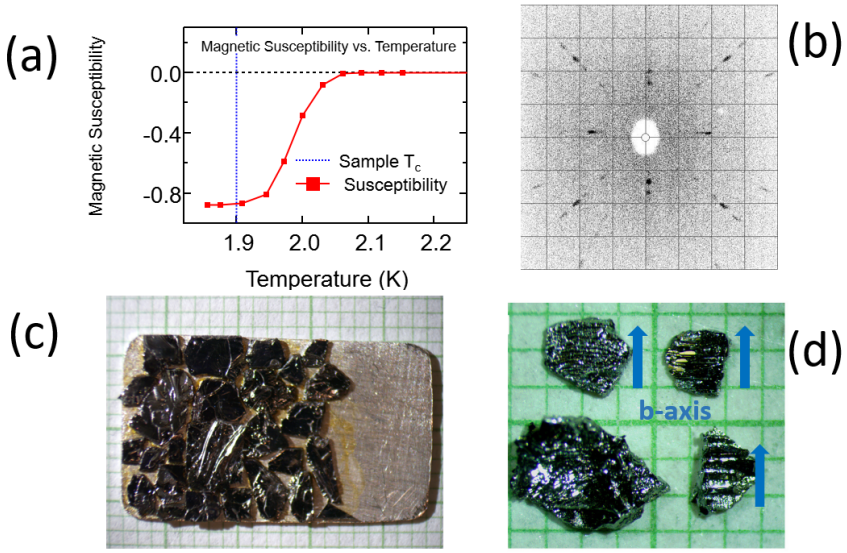

Figure 4: Panel (a) shows a plot of the magnetic susceptibility, χ, of $LaNiGa_2$ as a function of temperature. Well above T_c, susceptibility is 0; as temperature drops, the magnetic response increases. The lowest value reached of -0.88 indicates that about 88% of the sample is superconducting. Panel (b) shows a Laue diffraction pattern of $LaNiGa_2$. Such a pattern is dependent on crystallographic axis and thus aids in determining the orientation of a sample. Panel (c) shows the completed $LaNiGa_2$ mosaic with all samples aligned. Panel (d) shows terraced $LaNiGa_2$ samples, taken from source [1]. Compare with platelike samples shown in Figure 3: the b-axis grows along the length of these terraced crystals, setting them apart from their platelike counterparts.

3.2 Resistivity Measurements

As described in section 1.3, measuring resistivity can provide evidence of superconductivity and information about sample quality. An ideal sample for resistivity measurements is one shaped like a rectangular prism. That is because resistivity is not measured directly; instead, current is driven through the sample and the resulting resistance is calculated by measuring the potential difference between two points and employing Ohm's Law, V = IR or R = V/I. Resistivity is then calculated from the equation $\rho = RA/L$ where R is resistivity from the previous equation, A is the cross-sectional area of the sample, and L is the separation between the points of contact in the resistance measurement. In a sample that is a neat rectangular prism, it is easy to measure A and L with small uncertainty. The resistivity value obtained from this equation is given

in units of Ω*m, and should be the same throughout an entire sample, regardless of where the measurement is taken.

The first step in taking a resistivity measurement is selecting a sample, ideally with a uniform cross-sectional area. The cross-sectional area is then calculated by multiplying the thickness and the depth of the sample. The next step is to attach leads (small wires) to the sample. Using two-part silver epoxy (EPO-TEK H20E) combined in equal proportions by weight, 4 platinum leads are annealed and then laid on the sample. The so-called "four lead method" is the best way to measure resistivity in a sample because the outermost leads drive current while the inner leads measure resistance. An ideal voltmeter (which is the purpose of the inner leads) has infinite resistance, but it is impossible to drive a current through leads with very high resistance. This setup allows for high resistance to remain between the inner leads while current passes through the sample from the outer leads, for more details see [3]. The lead placement inherently causes uncertainty in resistivity values: current will travel between any conductive surfaces it can, and since the epoxy used to fix leads is conductive, excess epoxy can artificially shorten the distance between leads. Uncertainty values based on measurements of possible current paths through a sample are presented in Table 1 and Figure 5.

After four leads are laid along the length of the sample, the epoxy is cured by placing the sample in an evacuated oven and heating the oven to about 150 C for half an hour. Then, the leads are soldered to a measurement puck compatible with the Physical Property Measurement System (PPMS). When a material is likely superconducting and low resistivity values will be measured, an AC current supply should be used; this corresponds to an AC measurement puck [3]. Once soldering is complete, a small amount of current is driven through the soldered connections to anneal any excess solder away [3]. The measurement puck is then implanted in the PPMS, where resistivity is measured between 300 and 1.9 K.

Resistivity measurements were taken for nine samples of $LaNiGa_2$ total. Five of these came from batch DZ 424, two came from DZ 414, and one came from both DZ 465 and DZ 482. As found in previous resistivity measurements of $LaNiGa_2$, results varied significantly between different samples. RRR values, defined as $\rho(300\text{ K})/\rho_0$, ranged between 10.7 and 14.2. ρ_0 values varied between 3.9 and 8.4 $\mu\Omega$*cm (more than a factor of 2) and $\rho(300\text{ K})$ varied between 44 and 94 $\mu\Omega$*cm (also more than a factor of 2). T_c was not consistent between samples either: some samples became superconducting at 2.03 K, another still displayed nonzero resistivity at 1.9 K, the lowest temperature achievable in the PPMS. Even samples from the same batch lacked consistency: both extreme RRR values came from DZ 424, as well as both extreme T_c values (2.03 K and no superconductivity at 1.9 K). In short, the perplexing results of initial investigations into $LaNiGa_2$ resistivity are reflected here.

One possible explanation is that resistivity in $LaNiGa_2$ is anisotropic: that is, resistivity is different along

Sample	T_c–based on PPMS (K)	RRR	ρ_0 (μΩ*cm)	ρ(300 K) (μΩ*cm)	χ	T_c–based on MPMS (K)
DZ 414 S1	2.03	11.0	6.0 ± 0.7	67 ± 7		
DZ 414 S2	2.01	11.3	8.4 ± 0.6	95 ± 7		
DZ 424 S1	< 1.9	14.2	3.0 ± 0.2	44 ± 3	-0.88	1.87
DZ 424 S2	1.90	12.0	4.0 ± 0.4	51 ± 5	-0.98	1.9
DZ 424 S3	2.02	10.2	7 ± 1	80 ± 10	-0.96	1.85[a]
DZ 424 S4	2.02	12.1	3.9 ± 0.4	46 ± 5		
DZ 424 S5	2.00	12.5	7.0 ± 0.6	87 ± 7		
DZ 465	< 1.9	11.2	6.0 ± 0.7	64 ± 7	-1	1.88
DZ 482	1.9	10.7	5.6 ± 0.8	60 ± 8	-1	1.88

[a] T_c does not align between measurement methods for this sample. The cause of this discrepancy is unknown, but it is unexpected. All other samples show relative agreement in Tc between measurement methods.

Figure 5: This table shows parameter values for the nine samples whose resistivity was measured. Included are T_c, RRR, ρ_0, and ρ(300 K). For five of the samples, magnetic susceptibility was measured as well. These values are given where measured, along with T_c as determined from MPMS measurements.

different crystallographic axes. This could explain the significant discrepancy in RRR, ρ_0, and even T_c values obtained between samples: resistivity might have been measured along different crystallographic axes. If resistivity is indeed anisotropic, then resistivity values would be orientation-dependent and likely different between samples, since aligning along crystallographic axis did not take place prior to lead placement and measurement. There is a precedent for different materials displaying resistivity anisotropy, Walmsley and Fisher (2017) even provide a quantitative framework for measuring resistivity anisotropy in materials with orthorhombic unit cells like $LaNiGa_2$ [5]. Resistivity anisotropy often coincides with limited symmetry, and the unit cell of $LaNiGa_2$ has few conventional symmetries in lieu of glide plane and screw axis symmetries, as described in section 1.1. Potential resistivity anisotropy also hints at the possibility of anisotropic defect placement. Since RRR values indicate sample purity, they would be expected to be similar between samples from the same batch, even if ρ_0 is different—the flux growth process is homogenous and thus defects should affect all crystals from the same batch equally. However, if resistivity is anisotropic, so too could be the placement of impurities. As $LaNiGa_2$ crystals are nucleating, certain spots in the unit cell could be less stable or more electronegative, causing them to seek out and establish bonds with impurities like oxides or other elements deviating from their typical placement in the crystal. If this is the case, impurities would likely be found at specific, regular places in the crystal, and would possibly affect current flow in one direction but not a perpendicular direction to the first.

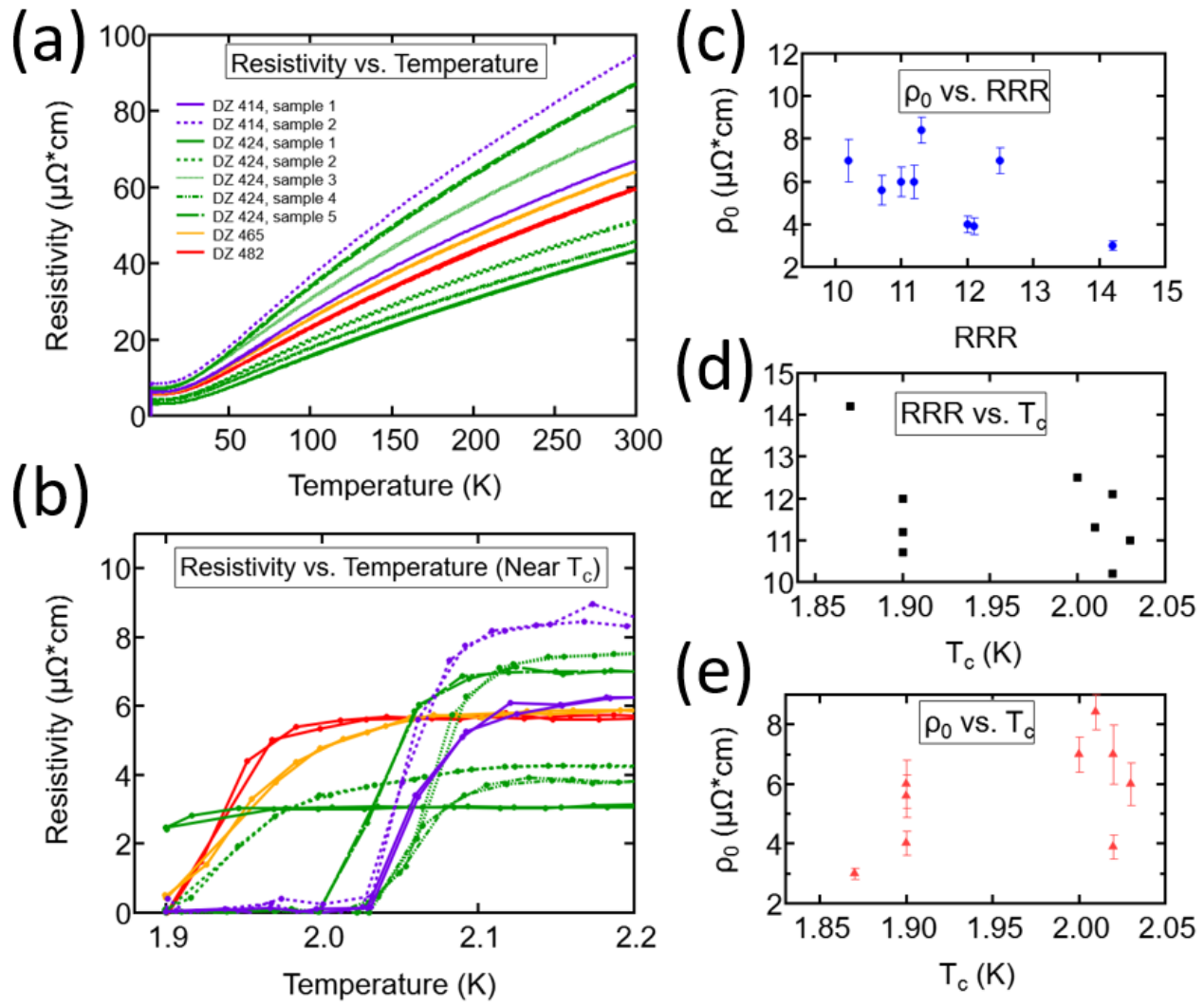

Figure 6: Panels (a) and (b) show resistivity as a function of temperature. Panel (a) shows the full temperature range measured, between 1.9 and 300 K, panel (b) shows only temperatures near T_c. From these plots, it is evident that resistivity varies widely between samples at both high and low temperatures, even between samples from the same batch. Panel (c) shows ρ_0 as a function of RRR—each point corresponds to a sample. Lower RRR values correlate with higher ρ_0 values since RRR is inversely proportional to ρ_0 by definition. Panels (d) and (e) show RRR vs. T_c and ρ_0 vs. T_c, respectively. Error bars show uncertainty values based on lead attachment to samples, described in the main portion of the paper. There is no clear correlation between resistivity and T_c in plots (c), (d), and (e). This, combined with the differences in resistivity as a function of temperature even for samples from the same batch, supports anisotropic resistivity in $LaNiGa_2$.

To better understand the resistivity of $LaNiGa_2$, more resistivity measurements need to be taken. Specifically, samples need to be aligned before their resistivity is measured. Samples from the same batch that share the same alignment should have identical values for RRR, ρ_0, and T_c. Ideally, samples from different batches should have identical values as long as they are properly aligned. If this is the case, a next step would be to measure resistivity along each crystallographic axis, quantify resistivity anisotropy, and hopefully, gain an understanding of how constituent atoms may affect resistivity differently. Completing these measurements is also a next step in understanding how $LaNiGa_2$ crystals nucleate during flux growth, and whether defects occur at random in the unit cell or if certain spots are more prone to hosting impurities.

4 Conclusions and Future Work

$LaNiGa_2$ is an unconventional, TRS-breaking superconductor thanks to symmetries in the crystal's unit cell [1]. The symmetries in $LaNiGa_2$ create degeneracies in the band structure, which in turn enable an unconventional superconducting electron pairing state to form. The band degeneracies (so-called topological features) along with superconductivity make $LaNiGa_2$ (and other potential similar materials) into possible host materials for Majorana fermions, elusive particles of great promise to quantum computing. The recently implemented single-crystal flux growth technique for $LaNiGa_2$ shed light on the internal structure of the material, revealing a *Cmcm* unit cell [1]. The macroscopic order of single crystal samples compared to their polycrystalline counterparts (in which unit cells are not all aligned) will likely enable a greater understanding of the material, since more precise experiments will be possible.

My work at UC Davis in the Taufour Lab this summer focused on three major goals. First, I attempted to synthesize single crystal samples of $LaNiGa_2$ from elemental starting materials. The synthesis process is described in detail in Section 2, but ultimately, all three synthesis attempts proved unsuccessful. $LaNiGa_2$ growth is extremely sensitive to the stoichiometry of precursors as well as to temperature gradients within a furnace and temperature differences between furnaces. Adjusting the stoichiometry of precursors even by a small amount can cause an entirely different compound (like $LaGa_2$) to form, while temperature discrepancies can change the nucleation, structure, and physical properties of $LaNiGa_2$ crystals. Second, I helped prepare a mosaic of $LaNiGa_2$ crystals for an experiment using μSR to detect the TRS-breaking internal magnetic field, as described in Section 3.1. Preparing the mosaic involved selecting samples of adequate dimensions and measuring the magnetic susceptibility to gain a sense of a sample's bulk superconductivity. The completed mosaic contained 24 crystals and was sent to collaborators in Canada in early August 2022. Finally, I measured the resistivity of $LaNiGa_2$ crystals. The initial goal of this project was to obtain many samples of uniform resistivity to use in a study on the effects of electron irradiation on resistivity, but this proved

unrealistic. As was found in a previous examination of $LaNiGa_2$ resistivity, RRR, ρ_0, and T_c values varied significantly between different the nine samples measured. This hints at the possibility of anisotropies in $LaNiGa_2$ in both resistivity and the placement of impurities.

Future work with $LaNiGa_2$ should involve a deeper investigation of resistivity. To check for resistivity anisotropy, samples should be aligned via Laue diffraction before measurement takes place. If resistivity anisotropy is present, a comparison of RRR values at different crystallographic orientations may help reveal possible anisotropies in the placement of impurities in $LaNiGa_2$. Prior to further study of resistivity, however, it is crucial to better understand the $LaNiGa_2$ synthesis process—specifically, the impact of temperature on crystal nucleation and crystallographic orientation at the macroscopic scale. Taking this step is paramount to being able to produce platelike samples of $LaNiGa_2$, which display better physical qualities and are more orderly than terraced samples. Unfortunately, given the number of uncontrollable variables during synthesis and furnace operation, understanding the role of temperature is largely a matter of trial and error. Reproducibility of high-quality samples of $LaNiGa_2$ is key to propelling ongoing research forward, so this issue must be solved. Given that $LaNiGa_2$ has just recently been produced in high quality single-crystal form, understanding of the material and its properties is still limited [1]. Other intermetallic compounds with similar unit cell structure may have similar properties, including both topological features and superconductivity. Therefore, an improved understanding of $LaNiGa_2$, the nature of its TRS-breaking, its resistivity, and other traits may promote understanding of other materials as well.

References

[1] Badger, J.R., Quan, Y., Staab, M.C. et al. Dirac lines and loop at the Fermi level in the time-reversal symmetry breaking superconductor $LaNiGa_2$. Commun Phys 5, 22 (2022). https://doi.org/10.1038/s42005-021-00771-5

[2] Kittel, C. Introduction to Solid State Physics, (John Wiley & Sons, New Jersey, 2005), 8th ed., Chapter 10. ISBN: 0-471-41526-X

[3] Badger, J.R. Structural Characterization and Physical Properties of Superconducting $LaNiGa_2$ and Antiferromagnetic CeIn3. [Doctoral Dissertation, University of California, Davis], 2021. https://escholarship.org/uc/item/6sz539tw

[4] Hillier, A.D. et al. Nonunitary triplet pairing in the centrosymmetric superconductor LaNiGa2. Phys Rev Lett. 2012 Aug 31;109(9):097001. doi: 10.1103/PhysRevLett.109.097001. Epub 2012 Aug 27. PMID: 23002872.

[5] Walmsley, P., and Fisher, I. R. Determination of the resistivity anisotropy of orthorhombic materials via transverse resistivity measurements. Rev Sci Instr 88, 043901 (2017). https://doi.org/10.1063/1.4978908